A Microwave Ferrite Single-Sideband Modulator*

ALVIN CLAVIN†, SENIOR MEMBER, IRE

Summary—A microwave single-sideband modulator has been designed utilizing two reflection types of Faraday rotation ferrite-balanced modulators. Power is fed to the two balanced modulators by means of a 3-db quadrature hybrid such that each modulator has equal incident power with a 90-degree phase difference. The output power of the balanced modulators is combined by means of a magic tee sum and difference circuit. It is shown that if the modulation signals applied to the balanced modulators are in phase quadrature, the upper sideband will appear at the output sum arm and the lower sideband will appear in the output difference arm. An analysis of the device relates the spurious and undesired sidebands to the conversion loss, and a method is proposed for minimizing carrier output. The drive power is reduced due to the use of reflection-type balanced modulators, and experimental data is presented for the modulation frequency impedance and drive power requirements. The temperature and frequency sensitivity of the undesired sidebands have also been measured. A number of applications of the device are discussed.

Introduction

SINCE THE advent of Doppler and pulse Doppler types of radar systems, a need has arisen for a means to simulate signals received from moving targets. Phase-coherent Doppler signals can be generated by single-sideband techniques which effectively translate the input frequency to the desired Doppler frequency. The type of circuit covered in this paper is similar to circuits used in the past at lower frequencies, and provides for summing two balanced-modulator outputs. The first work reported on a modulator of this type at microwave frequencies was due to Cacheris[1] who reported on a two- and three-phase system.

The circuit to be utilized, as shown in Fig. 1, consists essentially of a power splitter, a microwave phase shifter, two balanced modulators, and an output sum-and-difference circuit. The heart of the device is the balanced modulator which will be described in detail. Then the entire circuit of Fig. 1 is discussed and finally the problem of carrier suppression is presented. Experimental results verify the theory, and data is presented showing drive power requirements as well as temperature and frequency behavior.

Balanced Modulator

The balanced modulator chosen for this application utilizes the principle of Faraday rotation of the plane of polarization of microwave energy when passing through magnetized ferrite and is shown in Fig. 2. The balanced modulator consists of several parts: first, an orthogonal mode junction which has the property that arbitrarily polarized energy traveling in a circular waveguide will couple to either of two orthogonal rectangular waveguide outputs in an amount dependent upon the polarization angle; second, a ferrite section which is terminated in a short-circuit plate. When magnetized, the ferrite will rotate the polarization of the energy proportional to the applied field below saturation of the material. Since the Faraday rotation is nonreciprocal, the shorting plate in reflecting the microwave energy back through the ferrite causes a doubling of the rotation angle. This reflection modulator is very efficient since the ferrite and coil are only half as long as they would be if the reflection technique were not used. This gives a modulation power-saving feature to the unit.

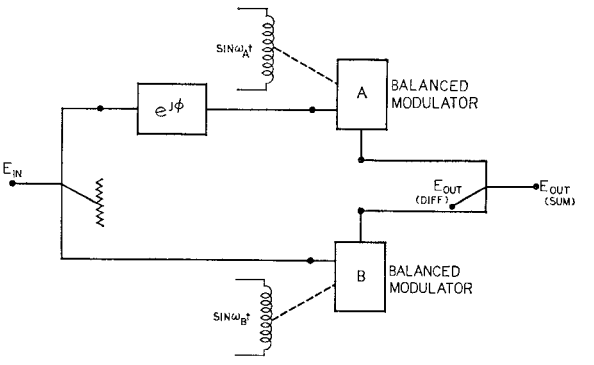

Fig. 1—Single-sideband modulator circuit. For proper operation, $e^{j\phi}=e^{j\pi/2}$, $\omega_A=\omega_B+\pi/2$.

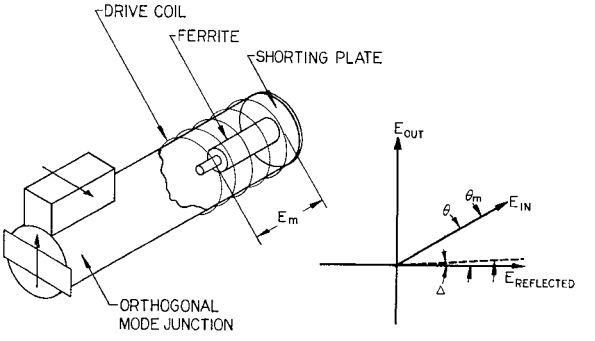

Fig. 2—Balanced modulator and phasor diagram showing component parts and polarization relationships.

Referring to Fig. 2, it is seen that

$$E_{out} = E_{in}e^{j\omega_0 t}(K_A + \sin\theta), \tag{1}$$

where

K_A = carrier leakage constant (indicates portion of input which leaks to the output),
θ = polarization rotation angle.
ω_0 = RF angular frequency

* Received by the PGMTT, April 19, 1961; revised manuscript received, June 20, 1961.
† Microwave Dept., Rantec Corporation, Calabasas, Calif.
[1] J. C. Cacheris, *et al.*, U. S. Patent No. 2,896,172; July 21, 1959.

Let us assume sinusoidal modulation such that

$$\theta = \Delta + \theta_m \sin \omega_m t, \tag{2}$$

where

Δ = bias angle (Δ is small and usually due to hysteresis),
ω_m = angular modulation frequency,
θ_m = maximum rotation angle.

Substituting (2) into (1) and expanding, one obtains

$$E_{\text{out}} = E_{\text{in}} e^{j\omega_0 t}[K_A + \sin \Delta \cos (\theta_m \sin \omega_m t) + \cos \Delta \sin (\theta_m \sin \omega_m t)]. \tag{3}$$

Assume Δ is small so that

$$\sin \Delta \cong \Delta$$

$$\cos \Delta \cong 1$$

and expanding in a series expression,

$$E_{\text{out}} = E_{\text{in}} e^{j\omega_0 t}\{K_A + \Delta[J_0(\theta_m) + 2(J_2(\theta_m) \sin 2\omega_m t + J_4(\theta_m) \sin 4\omega_m t + \cdots)] + 2[J_1(\theta_m) \sin \omega_m t + J_3(\theta_m) \sin 3\omega_m t + \cdots]\}. \tag{4}$$

By inspection of (4) one sees that if Δ is very small there is no carrier (outside of leakage) or even order harmonics, and only odd harmonics are present.

Sideband Ratios

In order to determine the "cleanness" of the spectrum output let us assume for the moment that Δ and K_A equal zero in (4) so that only first and third harmonics are present. The amplitude ratios of these sidebands are

$$\frac{J_1(\theta_m)}{J_3(\theta_m)}.$$

The conversion loss for this condition is from (4),

$$\frac{E_{\text{out}}}{E_{\text{in}}} = 2J_1(\theta_m) \sin \omega_m t = jJ_1(\theta_m)[e^{j\omega_m t} - e^{-j\omega_m t}]. \tag{5}$$

For a given conversion loss θ_m can be obtained from (5). The sideband ratio $J_1(\theta_m)/J_3(\theta_m)$ can then be computed. Fig. 3 shows a curve of sideband ratios for various conversion losses. The polarization rotation angle in degrees is noted on the curve.

Thus, it can be determined from Fig. 3 that, with a conversion loss of only 10 db, it is possible to obtain sideband discrimination of over 30 db, and if 20 db losses can be tolerated, higher-order sidebands are completely negligible, being greater than 55 db down.

Single-Sideband Circuit with Sinusoidal Modulation

Referring to the single-sideband general circuit of Fig. 1, it can be seen that the conditions necessary for a perfect single-sideband modulator can be approximated with the Faraday-rotation type by letting

$$e^{j\phi} = \pi/2 \quad \text{and letting} \quad \omega_A = \omega_B + \pi/2.$$

That is, the modulation phase of the A and B modulators is separated by 90°.

Let (2) represent the modulation character of the A modulator and let

$$\theta = \delta + \theta_m \cos \omega_m t \tag{6}$$

represent the modulation character of the B modulator so that,

$$E_A = E_{\text{in}} e^{j\omega_0 t}[K_A + \sin (\Delta + \theta_m \sin \omega_m t)] \tag{7}$$

$$E_B = E_{\text{in}} e^{j\omega_0 t}[K_B + \sin (\delta + \theta_m \cos \omega_m t)]. \tag{8}$$

As seen from Fig. 1,

$$E_{\text{in}} = j\frac{1}{\sqrt{2}} \quad \text{for the } A \text{ modulator,}$$

$$E_{\text{in}} = \frac{1}{\sqrt{2}} \quad \text{for the } B \text{ modulator,}$$

so that

$$\sqrt{2}[E_A \pm E_B] = j\frac{1}{\sqrt{2}} e^{j\omega_0 t}\{K_A + \Delta[J_0(\theta_m) + 2(J_0(\theta_m) \sin 2\omega_m t + J_4(\theta_m) \sin 4\omega_m t + \cdots)] + 2[J_1(\theta_m) \sin \omega_m t + J_3(\theta_m) \sin 3\omega_m t + \cdots]\} \pm \frac{1}{\sqrt{2}} e^{j\omega_0 t}\{K_B + \delta[J_0(\theta_m) + 2(-J_2(\theta_m) \cos 2\omega_m t + J_4(\theta_m) \cos 4\omega_m t \cdots)] + 2[J_1(\theta_m) \cos \omega_m t - J_3(\theta_m) \cos 3\omega_m t + \cdots]\}. \tag{9}$$

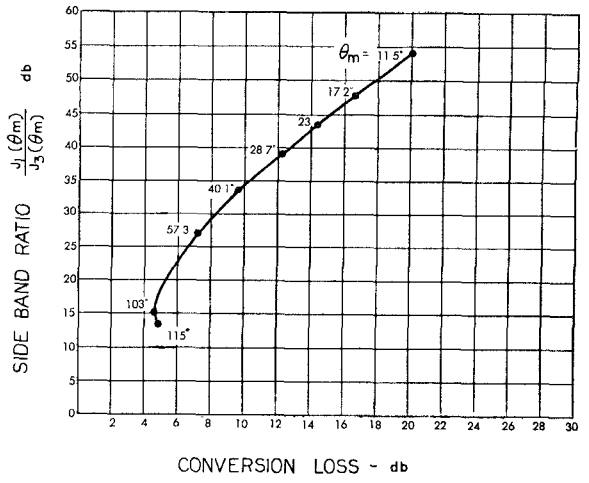

Fig. 3—Ratio of first-order to third-order sidebands as a function of conversion loss of balanced modulator, maximum polarization rotation angle noted on curve.

If Δ and δ are small and (θ_m) is less than 45°, higher harmonics can be neglected so that

$$(E_A \pm E_B) = \tfrac{1}{2}e^{j\omega_0 t}[(K_B \pm jK_A) + J_0(\theta_m)(\delta \pm j\Delta)] + J_1(\theta_m)\{[e^{j\omega_m t} - e^{-j\omega_m t}] \pm [e^{j\omega_m t} + e^{-j\omega_m t}]\}. \quad (10)$$

Simplifying g,

$$E_A \pm E_B = \pm J_1(\theta_m)e^{j(\omega_0 \pm \omega_m)} + \tfrac{1}{2}e^{j\omega_0 t}\{K_L + J_0(\theta_m)[\delta \pm j\Delta]\}, \quad (11)$$

where

$$K_L = (K_A + jK_B).$$

The first term indicates the desired single sideband and shows that the upper sideband appears only in the output sum arm and the lower sideband appears only in the difference arm. The sideband outputs are 180° out of phase with each other. The remaining terms represent carrier outputs and can be minimized by reduction of the values of δ and Δ. However, unless the leakage is zero, there will be a carrier at the output.

Carrier-Suppression Method

If only a single output is desired, the unwanted sideband can be terminated in a dummy load. Since the leakage from the two modulators is of arbitrary amplitude and phase, it can add at the output junction in any arbitrary ratio. That is, a portion will go to the dummy load terminating the output of the undesired sideband and the rest will go to the desired sideband output port. If the values of δ and Δ could be controlled, and used to cancel the leakage in the desired port, the problem would be solved.

Fig. 4 shows a phasor diagram indicating the proposed method of carrier cancellation. It is possible to control the values of δ and Δ by either a permanent or electromagnet. δ and Δ can be made either positive or negative individually by such control and the output carrier can be balanced out as indicated in the figure. The method of carrier suppression is similar to that of balancing any bridge and the adjustment first of one and then the other balanced modulator bias angle results in a carrier null.

Experimental Results

A ferrite single-sideband modulator was built having the form shown in Fig. 5, and utilized hybrid junctions covering the frequency range of 9.6–10.5 kMc. The unit was designed so that offset frequencies in excess of 100 kc could be obtained. In order to achieve offset frequencies this high, the "shorted turn effect" of the waveguide wall had to be eliminated. This was accomplished by inserting thin wall strips of less than 0.1 mil thickness into slots cut into the waveguide for the length of the modulation coil. The coil consists of 738 turns of No. 34 wire and was 1.3 inches long. Its impedance char-

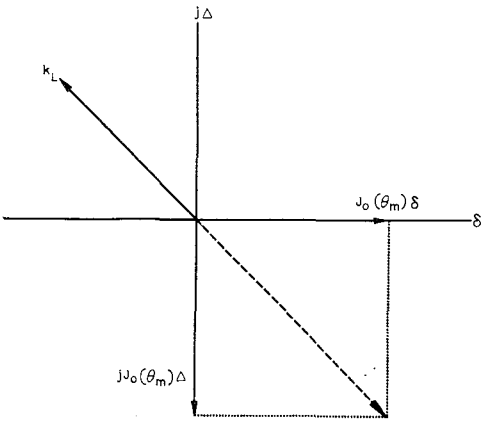

Fig. 4—Phasor diagram showing carrier components at output port with carrier suppressed.

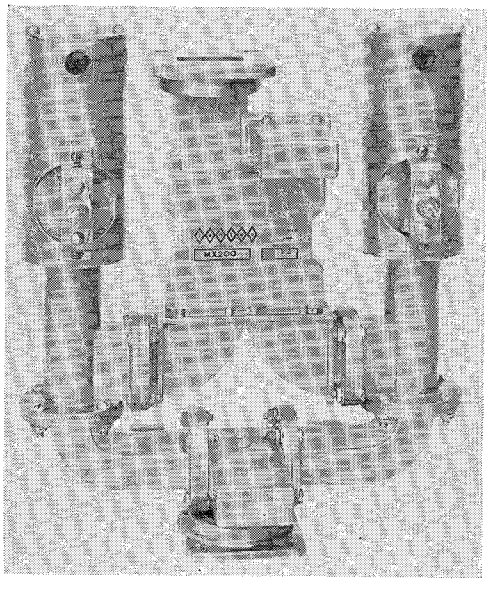

Fig. 5.

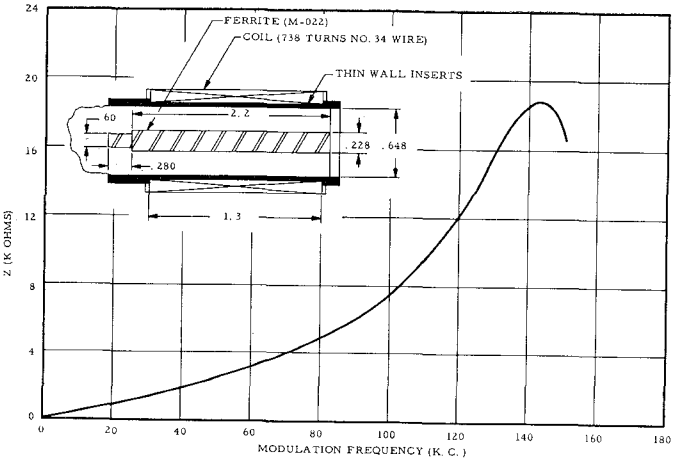

Fig. 6—Coil impedance as a function of modulation frequency. Ferrite and coil geometry as shown in insert.

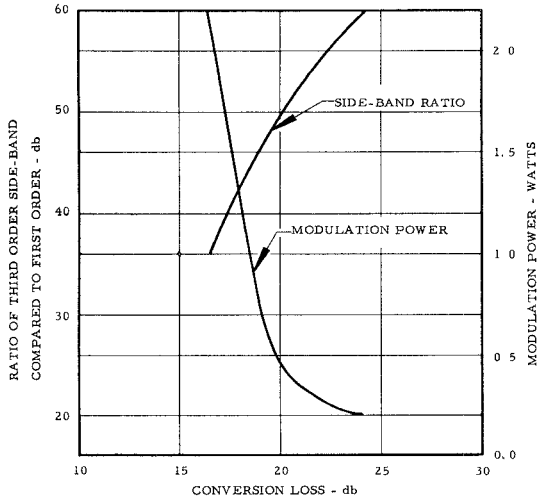

Fig. 7—Experimental characteristics of SSBM at $f_m = 60$ kc. Modulation power and sideband ratio vs conversion loss.

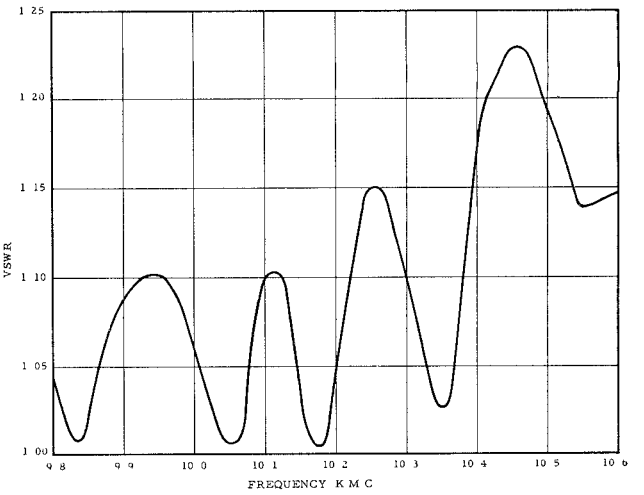

Fig. 10—Input VSWR vs frequency. Data obtained after carrier was suppressed from output.

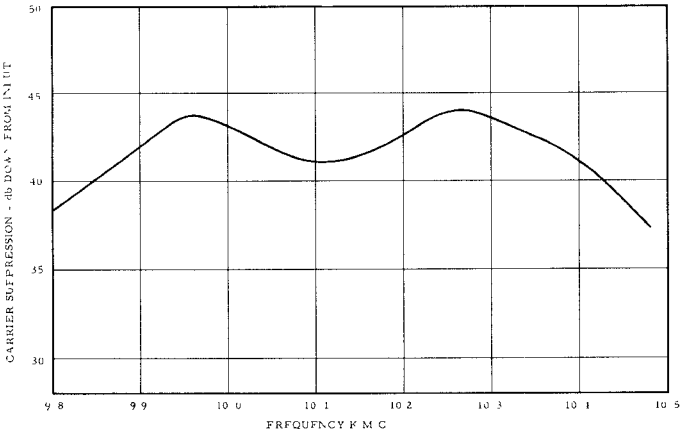

Fig. 8—Carrier suppression in db down from input vs frequency. Carrier tuned out for broad-band response by means of permanent magnets.

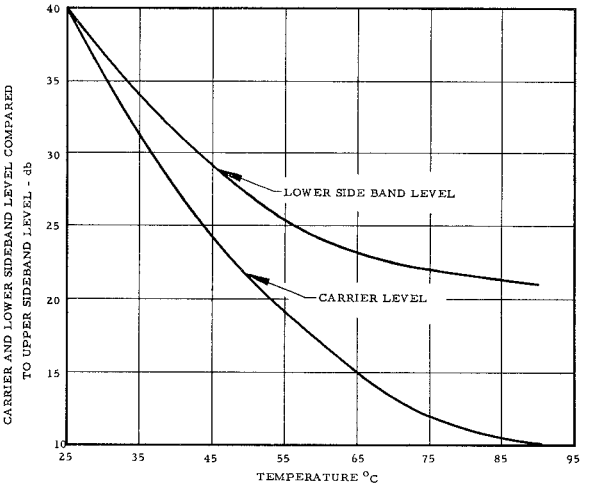

Fig. 11—Effect of increasing temperature on suppressed sidebands. No adjustment of bias angle or driver phase and relative amplitudes were made during temperature increase.

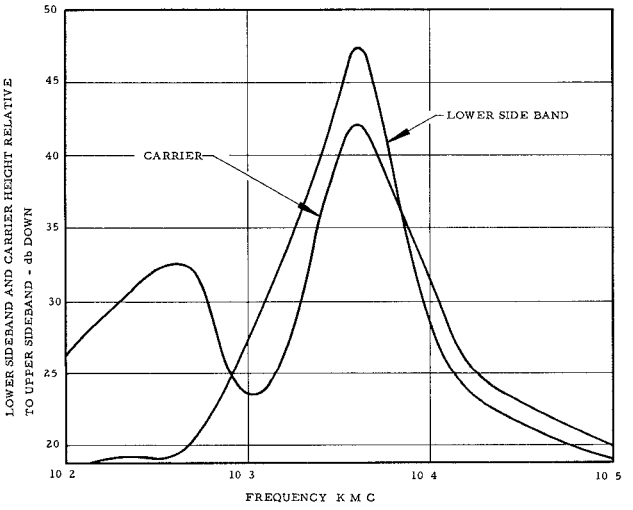

Fig. 9—Carrier and lower sideband level relative to upper sideband. Tuned for high suppression with resulting narrow bandwidth.

acteristic is shown in Fig. 6, and was obtained with the driver capacity across the coils. The self-resonant frequency was 140 kc ensuring good operation up to 100 kc. The ferrite utilized in the unit was Motorola M-022, and had the geometry shown in the inset of Fig. 6.

The driver contains two 5-watt amplifiers having a power splitting and phase shifting network at the input. The driver controls consist of an output voltage balance and phase adjustment as well as a level control which effects the gain of both amplifiers. In order to maintain 90° of phase shift over the entire modulation frequency band, there is a front panel switch which enables one to change capacitor values in the phase shift network. The driver is versatile and allows for easy adjustment of the single sideband modulator.

Fig. 7 shows the ratio of third-order to first-order sidebands obtained for the unit as well as the modulation power as a function of conversion loss for a modulation

frequency of 60 kc. The shape of the power curve is nonlinear since the conversion loss from (5) varies as $J_1(\theta_m)$. The sideband-ratio characteristic is similar to the theoretical curve of Fig. 3, but indicated higher-amplitude sidebands. The deviation becomes progressively worse as the conversion loss decreases. It is believed the deviation from the theoretical is due to distortion of the modulation amplifier waveform at high outputs. Since the SSBM is nearly linear, when third-harmonic distortion of the modulation current is present, a third-harmonic sideband will appear. Measurement of this harmonic content of the drive current was not attempted.

The amount of carrier suppression possible with the adjustment of the bias angles Δ and δ was next investigated. U-shaped bias magnets were mounted on the balanced modulators (see Fig. 5) in such a way as to be easily rotatable. The rotation angle varies the amount of longitudinal field, thereby adjusting the values of Δ and δ independently. Suppression of over 40 db relative to the input was obtainable from 9.9 to 10.5 kMc, as shown in Fig. 8. Better suppression can be obtained by careful adjustment of the magnets; however, at extremely low carrier outputs, the adjustment becomes quite critical. Such adjustment is shown in Fig. 9, where both carrier and lower sideband are adjusted to levels of over 40 db down from the upper sideband where the unit was operating with a conversion loss of 20 db. This high value of suppression can only be maintained for a narrow frequency band.

When the carrier is suppressed, the SSBM should still be matched. The reflections from the short circuit behind the modulators should combine into the dummy load adjacent to the input terminal on the quadrature hybrid. This is verified and the input VSWR is shown in Fig. 10. One should be able to maintain a low input VSWR if the modulator has been symmetrically constructed.

Temperature dependence of the modulator was next investigated. Conversion loss was uneffected by temperature changes; however, the sideband ratios changed markedly. This effect is shown in Fig. 11. The carrier and lower sideband were suppressed to 40 db relative to the upper sideband. The unit was placed in an oven and sideband ratios were measured with temperature increases. The carrier rose more radically than the lower sideband. Since the Faraday rotation is a function of temperature, it is not surprising that the values of Δ and δ are effected by such changes. However, operating temperatures below 50°C result in suppression of 20 db below the upper sideband.

Applications

Applications for the single-sideband modulator are numerous, the most common being the simulation of Doppler signals from moving targets. Other uses involve homodyne circuits for precision phase shift measurement and for the measurement of the insertion FM of a device. Phase-locked signal generators have been built, in which the single-sideband modulator acts as the local oscillator for a high-sensitivity receiver. In fact, the phase coherence of this device makes possible the arraying of a number of these units to feed a linear array of radiating elements. The single-sideband modulator offset frequency can be used to program the antenna beam position in space. The antenna beam in this array can be used for either searching or tracking by proper control of the single-sideband modulator.

Conclusions

A single-sideband modulator has been described which utilizes two Faraday-rotation types of balanced reflection modulators. The output spectrum of the device is free of harmonic sidebands, and carrier and lower sidebands are easily suppressed. The device is easily programable to various frequency-offsets, and offsets as high as 25 Mc have been obtained with good conversion efficiency. The device has numerous applications where phase-coherent signals are desired.

Acknowledgment

S. Rosen of the Rantec Electronic Laboratory has spent much time and effort in the study and construction of two phase-drivers for the single-sideband modulator. Without his efforts, these devices could not have been realized.